tabulated in Table I and plotted in Fig. 1. As can be seen, there is no significant difference from van Roosbroeck's theoretical results for large values of N, while for small N the fitting of the Monte Carlo values calculated by van Roosbroeck is much better.

The greatest differences can be observed in the region $N<50$. Since Y and F, deduced from experimental data for Ge and Si,[3] seem to correspond to values of N lying approximately between 10 and 70 (although the assumptions made on the value of E_i vary noticeably), these differences are interesting.

The program can be used for calculations with different values of the parameters, and, with little change, for further investigation. That is, the consequences of changes in the parameters β and γ, and of a probability distribution for the random cut x in the crazy-carpentry model, different from the uniform one, can be studied.

The authors wish to thank G. Bertolini and A. Rota for their suggestions and helpful discussions, and R. Meelhuysen for the FORTRAN programs.

[3] O. Meyer and H. J. Langmann, Nucl. Instr. Methods **39**, 119 (1966); S. O. W. Antman, D. A. Landis, and R. H. Pehl, *ibid.* **40**, 272 (1966); H. M. Mann, R. H. Bilger, and I. S. Shermann, IEEE Trans. Nucl. Sci. **NS13**, 252 (1966).

PHYSICAL REVIEW VOLUME 162, NUMBER 3 15 OCTOBER 1967

Reflectivity of Tin Telluride in the Infrared*

H. R. RIEDL, J. R. DIXON, AND R. B. SCHOOLAR
U. S. Naval Ordnance Laboratory, White Oak, Silver Spring, Maryland
(Received 17 May 1967)

The reflectivity of tin telluride at near-normal incidence and room temperature was measured at wavelengths from 1 to 200 μ. Thirteen single-crystal samples with free-hole concentrations ranging from 4.8×10^{19} cm^{-3} to 4.8×10^{20} cm^{-3} were studied. In the wavelength range from 3 to 200 μ, the results are well described by the classical theory of free-carrier dispersion. The free-carrier effective mass m_s, free-carrier optical mobility μ_{opt}, and optical dielectric constant ϵ_∞, which are parameters of the classical theory, were determined from curve fitting. These parameters are shown to be carrier-concentration-dependent. The dependence of m_s is indicative of a complex electronic band structure. The corresponding variation of ϵ_∞ is shown by a Kramers-Kronig–type analysis to be attributable to the Burstein shift of the fundamental absorption edge. For wavelengths less than 3μ, experimental reflectivities vary appreciably from those expected from free-carrier dispersion theory. It is shown that the deviations are the result of bound-carrier absorptions associated with the fundamental absorption edge.

I. INTRODUCTION

A RECENT analysis of the infrared reflectivity of SnTe has shown that the spectra from 3 to 10 μ can be satisfactorily represented by the classical theory of free-carrier dispersion.[1] The present investigation adds to this earlier study by extending (1) the number of carrier concentrations studied, (2) the analysis to include bound-carrier effects, and (3) the wavelength range to 200 μ.

II. EXPERIMENTAL

A. Bulk Samples

The samples were single crystals grown by Houston *et al.* of our laboratory.[2] Small rectangular parallelepipeds (approximately $1\times5\times0.8$ mm^3) were cut from single-crystal ingots. These small samples were heat treated by Houston to decrease the deviation from stoichiometry and, consequently, the extrinsic carrier concentration.

Values of the carrier concentration p, the Hall mobility μ_H, and the conductivity mobility μ_c were calculated using values of the weak-field Hall constant

TABLE I. The hole concentration $p=(0.6/R_He)_{77°K}$, Hall mobility $\mu_H=|R_H|\sigma$, and conductivity mobility $\mu_c=\sigma/(pe)$ for the optical samples.

Sample	p (10^{20} cm^{-3})	μ_H (10^2 cm^2/V sec) 300°K	μ_c (10^2 cm^2/V sec) 300°K
A	4.8	...	...
B	3.8	0.88	1.3
C	2.5	1.6	2.0
D	1.4	3.3	3.8
E	1.3	2.5	3.1
F	1.0	4.3	5.2
G	0.90	...	...
H	0.74	6.0	7.6
I	0.56	7.8	10.
J	0.55	7.6	10.
K	0.51	8.5	11.
L	0.48	9.1	12.

* A preliminary report of this subject was presented at the 1966 Washington, D. C. meeting of the American Physical Society [Bull. Am. Phys. Soc. **11**, 348 (1966)].

[1] H. R. Riedl, J. R. Dixon, and R. B. Schoolar, Solid State Commun. **3**, 323 (1965).

[2] B. B. Houston, R. F. Bis, and E. Gubner, Bull. Am. Phys. Soc. **6**, 436 (1961).

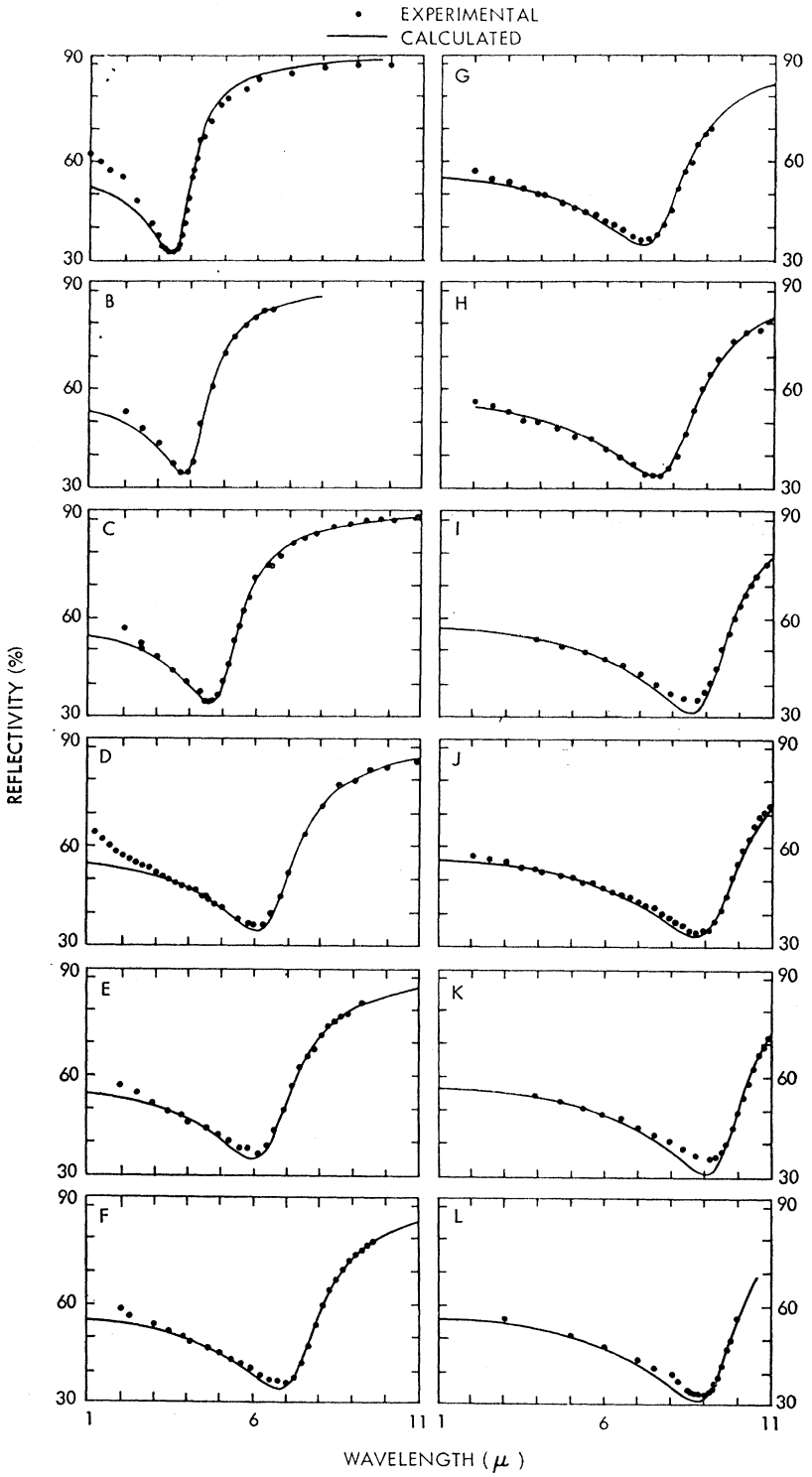

FIG. 1. Experimental and calculated reflectivity spectra for samples at room temperature listed in Table I. The letter on each plot corresponds to the letter used in Table I to identify samples. The calculated curves based upon Eqs. (1), (2), (5), and (6) represent only the free-carrier dispersion.

R_H, the factor[3] $r=0.6$, the conductivity σ, and the relations $p=(r/R_He)_{77°K}$, $\mu_H=|R_H|\sigma$, and $\mu_c=\sigma/(pe)$. Table I lists the samples and their electrical properties.

[3] B. B. Houston, R. S. Allgaier, J. Babiskin, and P. G. Siebenmann, Bull. Am. Phys. Soc. 9, 60 (1964).

To prepare these samples for reflection measurements, the largest face was polished using the procedure and etch developed by Norr.[4] Surfaces prepared by this

[4] M. K. Norr, J. Electrochem. Soc. 113, 621 (1966).

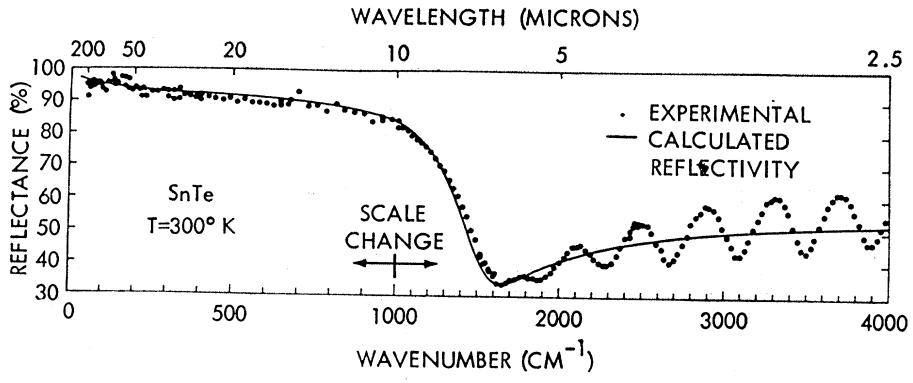

FIG. 2. The far-infrared reflectance of a single-crystal film on a NaCl backing at room temperature. The calculated curve is an extension of the single-surface reflectivity curve that fits the data for sample D shown in Fig. 1(D). This curve takes only free-carrier dispersion into account. The oscillations at short wavelengths are interference fringes.

method are flat and mirrorlike in appearance. X-ray analysis has shown them to be free of major strains.

Reflectivity measurements were made at room temperature using a Perkin-Elmer Model 112 spectrometer equipped with a LiF or NaCl prism. Measurements on such small samples were possible by using a reflectometer[5] which focused the image of the exit slit of the monochromator onto the sample at an angle of incidence of about 10° off normal. The image of the slit on the sample was 0.4×2 mm or smaller. The reflected intensity from the sample was compared to that of an aluminized mirror. Experimental reflectivities determined in this way were accurate to within about 3%.

B. Film Sample

One single-crystal film sample was used for reflectance measurements in the wavelength range 2.5 to 200 μ. The film was epitaxially grown as described in Ref. 6. Measurements were made using a Perkin-Elmer Model 301 grating spectrometer with a reflectance attachment in the entrance optics and an aluminized mirror for reference. The film, rather than one of the small bulk samples, was used for these measurements because the long-wavelength equipment requires samples with large-area reflecting surfaces. The film was 1 cm^2 in area and 1.4 μ thick, and had a hole concentration of 1.4×10^{20} cm^{-3}.

III. DISPERSION THEORY

The reflectivity at normal incidence is given in terms of the index of refraction n and the extinction coefficient κ by

$$R=[(n-1)^2+\kappa^2]/[(n+1)^2+\kappa^2], \quad (1)$$

and is related to the complex dielectric constant $\tilde{\epsilon}$ through the defining equations

$$\tilde{\epsilon}=\epsilon_1+i\epsilon_2=n^2-\kappa^2+i2n\kappa. \quad (2)$$

In terms of the contributions of bound carriers (BC), free carriers (FC), and lattice vibrations (LV), $\tilde{\epsilon}$ can be expressed as

$$\tilde{\epsilon}=\tilde{\epsilon}_{BC}+\tilde{\epsilon}_{FC}+\tilde{\epsilon}_{LV}. \quad (3)$$

If in the spectral region under investigation, $\tilde{\epsilon}_{LV}$ makes a relatively small contribution to $\tilde{\epsilon}$, then Eq. (3) becomes

$$\tilde{\epsilon}=\tilde{\epsilon}_{BC}+\tilde{\epsilon}_{FC}. \quad (4)$$

At the wavelengths somewhat beyond the fundamental absorption edge, $\tilde{\epsilon}_{BC}$ becomes independent of wavelength and is conventionally renamed the optical dielectric constant, ϵ_∞. In such a spectral region, therefore,[7]

$$\tilde{\epsilon}=\epsilon_\infty+\tilde{\epsilon}_{FC}. \quad (5)$$

According to classical theory, $\tilde{\epsilon}_{FC}$ is related to the free-carrier concentration N, electric-susceptibility effective mass m_s, and scattering time τ by

$$\tilde{\epsilon}_{FC}=-\frac{4\pi Ne^2}{m_s}\frac{1}{\omega^2+\gamma^2}\left(1-i\frac{\gamma}{\omega}\right), \quad (6)$$

where ω is the angular frequency of light and $\gamma=1/\tau$. This expression is in cgs units.

IV. RESULTS AND DISCUSSION

A. Free-Carrier Dispersion

Experimental and calculated reflectivity spectra for the bulk samples listed in Table I are shown in Fig. 1. The solid lines in Fig. 1 are calculated curves based upon Eqs. (1), (2), (5), and (6). The calculated curves were fitted to the experimental data by letting the optical dielectric constant ϵ_∞, the susceptibility effective mass m_s, and the optical mobility $\mu_{opt}=e\tau/m_s$ be the variable parameters.

The reflectance of an epitaxial film at room temperature is shown in Fig. 2. The film was chosen so as to have a carrier concentration very nearly equal to that of sample D. The solid curve represents the reflectivity calculated on the basis of classical free-carrier theory and the parameters applying to sample D. As such it represents an extension of the calculated curve drawn

[5] R. B. Schoolar and J. R. Dixon, Phys. Rev. **137**, A667 (1965).
[6] H. R. Riedl, R. B. Schoolar, and Bland Houston, Solid State Commun. 4, 399 (1966).
[7] F. Stern, in *Solid State Physics*, edited by F. Seitz and D. Turnbull (Academic Press Inc., New York, 1963), Vol. 15, p. 344.

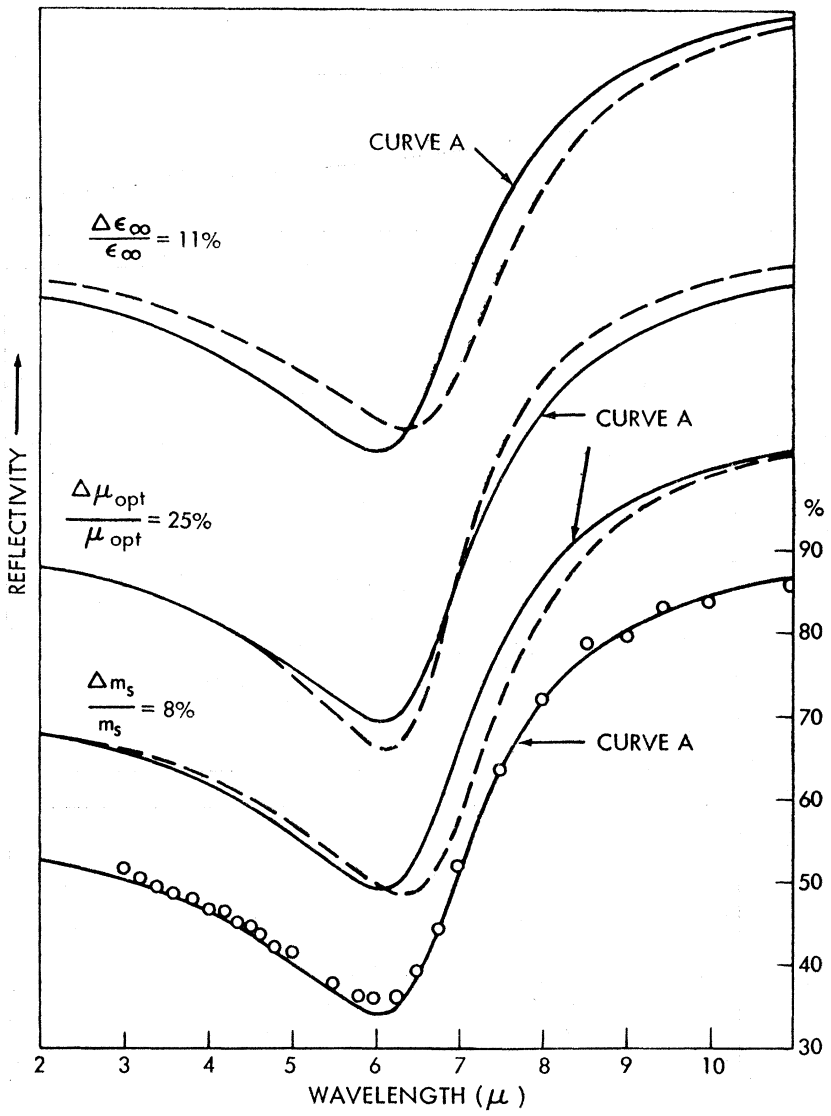

FIG. 3. Calculated curves showing the sensitivity to changes in the parameters used in curve fitting. The calculated curve A fits the data for sample D as shown at the bottom. The effect of changing one of the parameters is shown by each dashed curve. The reflectivity scale at the right applies to only the bottom curve and the experimental data. The other curves have been displayed vertically, in pairs, for clarity.

in Fig. 1(D). The agreement between experiment and calculation is remarkably good in the long-wavelength region where the reflectance of the film becomes equal to the reflectivity R of the material. At short wavelengths the reflectance oscillates about the calculated values of R because of interference effects, as expected. The good agreement between the calculations and the experimental data indicates that lattice dispersion does not contribute significantly to the reflectivity out to 200 μ. The relatively small role of lattice dispersion in this spectral region is consistent with the small values of the transverse and longitudinal optical mode frequencies which have been reported recently by Pawley *et al.*[8]

The sensitivity of the reflectivity to changes in the variables used in the calculations is demonstrated in Fig. 3. The solid curve fits the experimental data as shown at the bottom. The upper parts of the figure show the solid curve for reference and a broken curve indicating the effect of changes in each of the variables. Since each change has a rather unique effect on the reflectivity curve, the variables can be evaluated quite accurately. For instance, the estimated uncertainties associated with the curve fitting procedure, when applied to the data in Fig. 3, are 2% in ϵ_∞ and m_s and 10–15% in μ_{opt}. The source of error associated with uncertainties in values of carrier concentration was minimized by making the optical measurements on the Hall samples themselves. Over-all errors in ϵ_∞, m_s, and μ_{opt} are difficult to estimate but are probably fairly well represented by the scatter in the values.

Values of ϵ_∞, m_s, and μ_{opt} obtained from the curve fitting are all dependent upon carrier concentration,

[8] G. S. Pawley, W. Cochran, R. A. Cowley, and G. Dolling, Phys. Rev. Letters 17, 753 (1966).

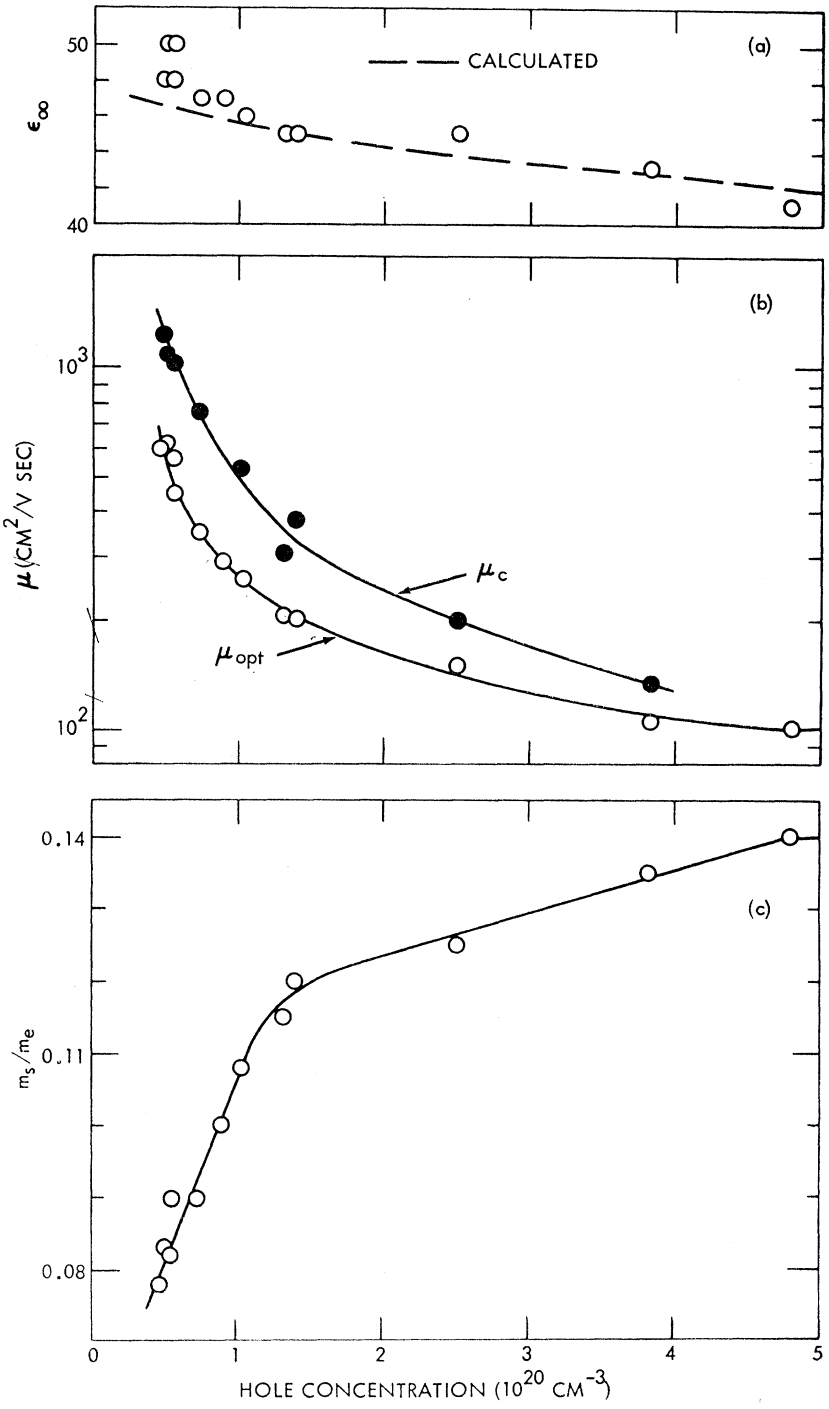

FIG. 4. Open circles represent values of the optical dielectric constant ϵ_∞, optical mobility μ_{opt}, and the susceptibility effective-mass ratio m_s/m_e, determined by fitting classical dispersion theory to room-temperature reflection spectra as shown in Fig. 1. In (a), the experimental values of ϵ_∞ are compared to a calculated curve as explained in the text. In (b) the optical mobility, $\mu_{opt}=e\tau/m_s$, is compared to the dc conductivity mobility, $\mu_c=\sigma/(pe)$.

as shown in Fig. 4. Finkenrath and Kohler have reported values[9,10] of ϵ_∞ over a large range of hole concentrations and a value[10] for m_s and for τ at $p^*=(1/R_He)_{300°K}=5\times10^{19}$ cm^{-3} $[p=(0.6/R_He)_{77°K}=3\text{–}4\times10^{19}$ cm$^{-3}]$. Their values for ϵ_∞ and τ are in agreement with ours, but m_s is substantially different. The discrepancy apparently results from their use of p^* rather than p to calculate m_s.[3]

The optical dielectric constant ϵ_∞, in Fig. 4 increases with decreasing hole concentration. The relationship between changes in the bound-carrier absorption spectrum and the corresponding changes in ϵ_∞ can be

[9] H. Finkenrath and H. Kohler, Phys. Letters 23, 437 (1966).
[10] H. Finkenrath and H. Kohler, Phys. Letters 24A, 261 (1967).

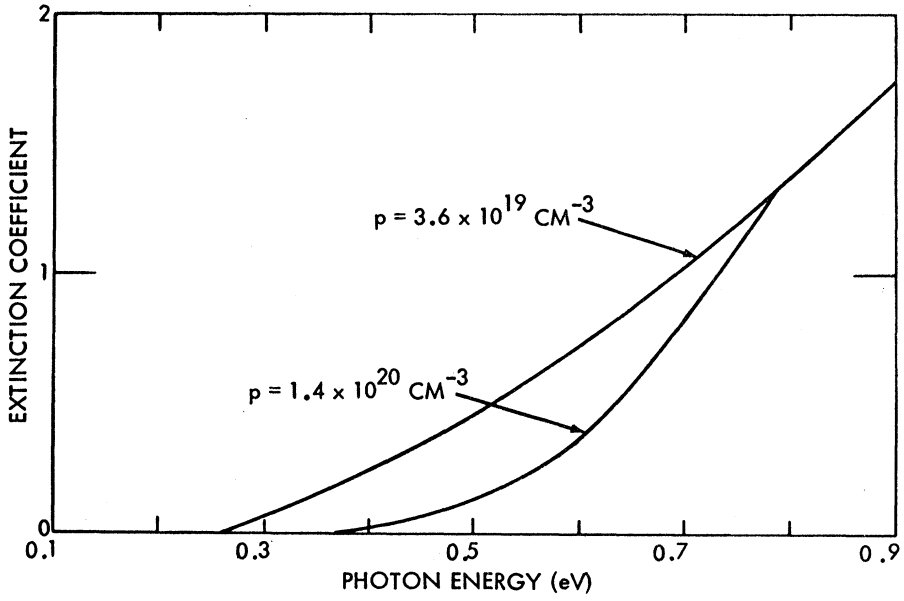

FIG. 5. Bound-carrier absorption spectra determined from transmittance and reflectance measurements at room temperature on epitaxial films with different carrier concentrations. See Ref. 12.

analyzed conveniently in terms of changes in the optical index-of-refraction $n_\infty=\sqrt{\epsilon_\infty}$. The Kramers-Kronig–type dispersion relation involved is[11]

$$\Delta n_\infty=\frac{2}{\pi}\int_0^\infty \Delta\kappa_{BC}(E')[E']^{-1}dE', \qquad (7)$$

where the absorption is expressed in terms of the extinction coefficient κ_{BC}. The integral is to be taken over all photon energies E' for which $\Delta\kappa_{BC}$ has nonzero values. Schoolar *et al.*[12] have obtained bound-carrier absorption spectra measured on epitaxial films at room temperature with hole concentrations ranging from 3.6×10^{19} to 6.8×10^{20} cm^{-3}. The absorption studies revealed significant shifts in the fundamental absorption edge with carrier concentration, presumably corresponding to the shift in the Fermi energy (Burstein shift).[13] Two of the curves from Ref. 12 are shown in Fig. 5. The changes in n_∞ corresponding to such observed shifts have been calculated for different carrier concentrations using Eq. (7). The calculations were performed relative to the κ_{BC} spectrum for $p=1.4\times10^{20}$ cm^{-3} and $n_\infty=(\sqrt{45.0})$. The results expressed in terms of ϵ_∞ are shown in Fig. 4(a) to agree with the experimental data to within the experimental error. Thus, the observed carrier concentration dependence of ϵ_∞ appears to be accounted for by the Burstein shift of the fundamental absorption edge. This result is in contrast to that reported for PbS.[14] For PbS the Burstein shift has been found to contribute very little to the observed carrier-concentration dependence of ϵ_∞.

The optical mobility is shown in comparison with the dc conductivity mobility in Fig. 4(b). Quantitative analysis of the expected relationship between these two properties could not be made. Such an analysis requires free-carrier scattering information not yet available for SnTe. It is interesting to note, however, that values of the optical mobility were also found to be smaller than the dc conductivity mobility in PbTe.[15]

The electric-susceptibility effective-mass ratio m_s/m_e is shown in Fig. 4(c) to be a strong function of carrier concentration. Values of m_s are governed by the band masses in the vicinity of the Fermi level. The observed variation, therefore, is indicative of a complex band structure. It should be noted that the variation in m_s shown in Fig. 4(c) changes rather abruptly at a hole concentration of about 1.3×10^{20} cm^{-3}. This is roughly the hole-concentration region for which anomalies in other properties have been observed.[16–20] For instance, the hole-concentration dependence of the thermoelectric power shows a minimum and the ratio of the room temperature to the low-temperature Hall coefficient shows a maximum in this region. These observations have been interpreted in terms the Fermi level passing into a second valence band. The abrupt change in m_s observed here could be the result of such a second band. However, the validity of this interpretation can

[11] Frank Stern, Phys. Rev. **133**, A1653 (1964).
[12] R. B. Schoolar, H. R. Riedl, and J. R. Dixon, Solid State Commun. **4**, 423 (1966), and unpublished results.
[13] E. Burstein, Phys. Rev. **93**, 632 (1954).
[14] J. R. Dixon and H. R. Riedl, Phys. Rev. **140**, A1283 (1965).
[15] J. R. Dixon and H. R. Riedl, Phys. Rev. **138**, A873 (1965).
[16] R. F. Brebrick and A. J. Strauss, Phys. Rev. **131**, 104 (1963).
[17] B. B. Houston and R. S. Allgaier, Bull. Am. Phys. Soc. **9**, 293 (1964).
[18] J. A. Kafalas, R. F. Brebrick, and A. J. Strauss, Appl. Phys. Letters **4**, 93 (1964).
[19] B. A. Efimova and L. A. Kolomoets, Fiz. Tverd. Tela **7**, 424 (1965) [English transl.: Soviet Phys.—Solid State **7**, 339 (1965)].
[20] B. A. Efimova, V. I. Kaidanov, B. Ya. Moizhes, and I. A. Chernik, Fiz. Tverd. Tela **7**, 2524 (1965) [English transl.: Soviet Phys.—Solid State **7**, 2032 (1966)].

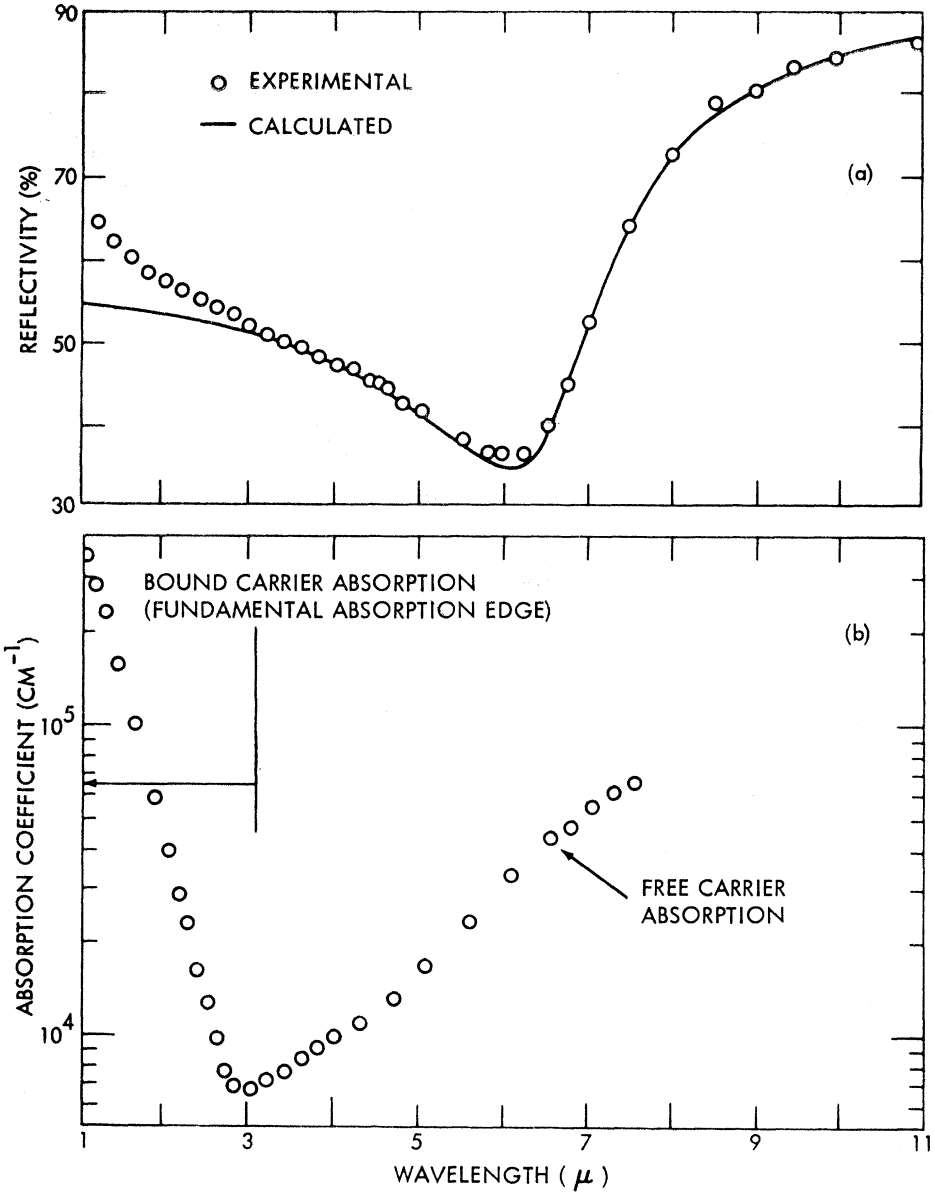

FIG. 6. (a) Experimental reflectivity spectrum of sample D at room temperature compared to calculated free-carrier reflectivity. (b) The absorption coefficient α, from transmittance and reflectance measurements on single-crystal films. The relationship between α, the extinction coefficient κ, and wavelength λ, is $\kappa=\alpha\lambda/4\pi$. Absorption data are from Ref. 12.

be verified only through a detailed analysis requiring band parameters not yet available for SnTe.

B. Bound-Carrier Dispersion

At wavelengths less than about 3 μ, the change in $\tilde{\epsilon}_{BC}$ significantly influences the reflectivity spectra. This is shown qualitatively in Fig. 6. In Fig. 6(a), the experimental reflectivity for sample D deviates from the calculated free-carrier curve at short wavelengths. Figure 6(b) shows the absorption spectrum[12] in the fundamental absorption-edge region. The absorption data were obtained from transmittance and reflectance measurements on single-crystal epitaxial films[6] with the same carrier concentration as sample D. It can be seen that the deviation of the experimental reflectivity from the calculated curve in Fig. 6(a) occurs in the same spectral region for which Fig. 6(b) shows strong bound-carrier absorption. The effects of bound carriers in this spectral region can also be seen in the data of Finkenrath and Kohler.[9] These authors obtained the optical constants associated with bound carriers by eliminating free-carrier effects from their data.

It should be noted from Fig. 6(a) that no peak in the reflectivity was observed at these short wavelengths. A peak in the index of refraction near the fundamental absorption edge has been observed in each of the related compound semiconductors PbS,[21,22] PbSe,[22]

[21] H. R. Riedl and R. B. Schoolar, Phys. Rev. **131**, 2082 (1963).
[22] J. N. Zemel, J. D. Jensen, and R. B. Schoolar, Phys. Rev. **140**, A330 (1965).

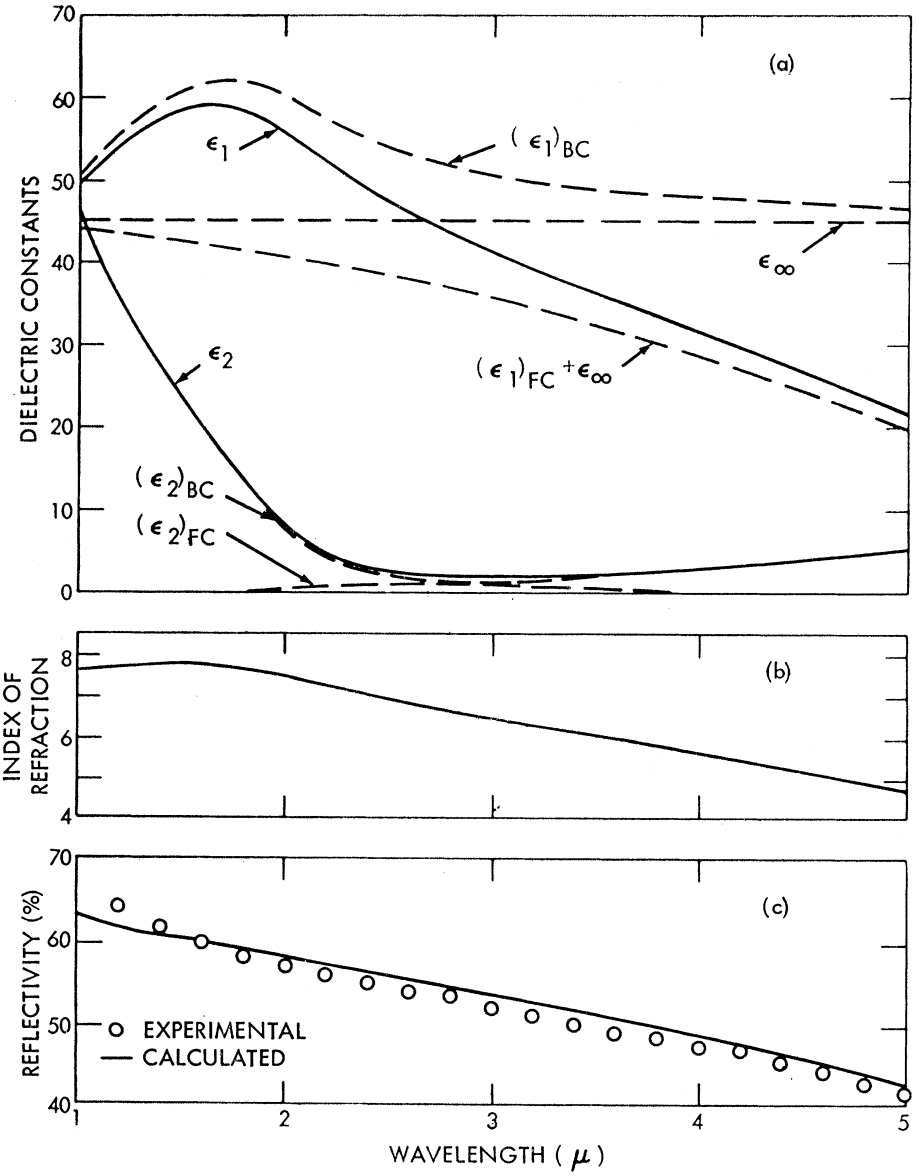

FIG. 7. Calculated curves applying to sample D of the dielectric constants (a), the refractive index (b), and the reflectivity (c). In (a) subscripts 1 and 2 refer to real and imaginary parts of the dielectric constant, respectively, and BC and FC refer to bound and free carrier, respectively. In (c) the calculated spectrum takes into account both bound- and free-carrier dispersion and is compared to the experimental room-temperature data for sample D.

and PbTe.[22] This results from the rapid change of the absorption in this spectral region.[5,11] It has been shown for PbS that this dispersion of the refractive index causes a small peak in the reflectivity spectrum.[21] Such peaks can easily be missed experimentally because of their smallness and also because of their sensitivity to surface conditions. For this reason we have carried out a Kramers-Kronig-type analysis to determine whether or not a peak larger than the scatter in the reflectivity data should have been observed for sample D. The analysis was based upon the bound-carrier absorption data corresponding to 1.4 $\times 10^{20}$ cm^{-3} shown in Fig. 5, the data of Schoolar *et al.*[12] out to 3 eV, and those of Cardona and Greenaway[23] from 3 to 20 eV. These data were used in conjunction with the dispersion relation[11]

$$n_{BC}(E)-1=(2/\pi)\int_0^\infty E'\kappa_{BC}(E')[E'^2-E^2]^{-1}dE' \quad (8)$$

and

$$\tilde{\epsilon}_{BC}=n_{BC}^2-\kappa_{BC}^2+i2n_{BC}\kappa_{BC}=(\epsilon_1)_{BC}+i(\epsilon_2)_{BC}, \quad (9)$$

to determine $(\epsilon_1)_{BC}$ and $(\epsilon_2)_{BC}$. These dielectric constants were combined with free-carrier contributions to obtain the total dielectric constants, as prescribed by Eq. (4). The values of $(\epsilon_1)_{FC}$ and $(\epsilon_2)_{FC}$ were obtained from the results described in Sec. IV *A*. The total dielectric constants were used to calculate the desired reflectivity spectrum.

[23] M. Cardona and D. L. Greenaway, Phys. Rev. 133, A1685 (1964).

In evaluating Eq. (8), the usable limits of integration are determined by the energy range over which κ_{BC} is known. In this case, the range is 0.3 to 20 eV. The unknown high-energy part of the integral was represented by a constant C added to the right side of Eq. (8). A value of $C=0.76$ was chosen so as to satisfy the requirement that $n_{BC}(E=0)$ be equal to $\sqrt{\epsilon_\infty}$. The value 45.0 was chosen for ϵ_∞ to agree with the result obtained from the free-carrier analysis of sample D. Values of the dielectric constants calculated as described above are presented in Fig. 7(a). The corresponding indices of refraction and reflectivities calculated from Eqs. (1) and (2) are presented in Figs. 7(b) and 7(c). The results of these calculations show that the refractive index exhibits a rather broad hump at short wavelengths, and that the structure in the reflectivity spectrum is too small to be observed in the data. In addition, the analyses show that the magnitude of the discrepancy between experimental and calculated reflectivities shown in Fig. 6(a) is well accounted for by bound-carrier effects.

V. SUMMARY

It has been shown that the infrared reflectivity of SnTe is a strong function of carrier concentration. All the spectra in the wavelength range from 3 to 200 μ are quantitatively accounted for in terms of the classical dispersion theory of free carriers. The optical dielectric constant ϵ_∞, the optical mobility μ_{opt}, and the susceptibility effective mass m_s are all functions of carrier concentration. The concentration dependence of ϵ_∞ appears to be accounted for by the Burstein shift of the fundamental absorption edge. The corresponding variation in m_s is indicative of a complex band structure. An abrupt change in m_s at $p\approx 1.3\times 10^{20}$ cm^{-3} could be the result of the second valence band suggested by other studies of thermal and electrical properties.

In the wavelength range 1 to 3 μ, the reflectivity is governed by contributions from both free and bound carriers. When both of these effects are taken into account, the experimentally observed reflectivity can be quantitatively accounted for.

ACKNOWLEDGMENTS

We wish to thank Dr. B. B. Houston, Dr. J. R. Burke, and Dr. R. S. Allgaier for supplying us with the bulk samples and the corresponding electrical properties and, for many stimulating discussions. We would also like to thank Dr. M. K. Norr for instructing us in the use of his polishing etch, and R. F. Bis for the use of his experimental data on samples A and L.

PHYSICAL REVIEW VOLUME 162, NUMBER 3 15 OCTOBER 1967

Electroreflectance Spectra due to Free Carriers in Semiconductors*

J. D. Axe and R. Hammer
IBM Watson Research Center, Yorktown Heights, New York
(Received 15 May 1967)

The modulation of the spectral reflectivity of a semiconductor-electrolyte interface has been observed in the deep infrared (200–600 cm^{-1}). In n-type Ge and GaAs the resulting electroreflectance spectra show pronounced characteristic structure, with peak modulation of several percent. These observations can be understood as resulting from a depletion region of variable thickness at the semiconductor interface which acts as a dielectric optical coating. More detailed considerations predict "resonances" in the modulation near lattice reststrahl and free-carrier plasma frequencies, as observed.

THE modulation of the spectral reflectivity of semiconductors by the application of alternating voltages to a semiconductor-electrolyte interface provides useful information concerning electronic interband transitions.[1] The method has until the present been limited to spectral regions in which common electrolyte solutions are reasonably transparent. We have extended electroreflectance studies into the deep infrared spectral region and wish to report here the first observation of electroreflectance "anomalies" due to modulation of free carriers in both polar and nonpolar semiconductors.[2,3]

The sample cell arrangement is essentially similar to those used in the visible spectral region. Thin ($\frac{1}{4}$ mil) dielectric spacers between the silicon window and the semiconductor surface reduced the optical

* Partially supported by Army Research Office, Durham, North Carolina.

[1] K. L. Shaklee, F. H. Pollak, and M. Cardona, Phys. Rev. Letters **15**, 883 (1965).

[2] L. Sosnowski, [Phys. Rev. **107**, 1193 (1957)] was very probably incorrect in attributing reflectivity modulation near the band gap in Ge to free carriers. B. O. Seraphin, R. B. Hass, and N. Bottka, [J. Appl. Phys. **36**, 2242 (1965)] have made a careful study of these effects and conclude that interband transitions are responsible (Franz-Keldysh effect).

[3] There have been numerous useful studies involving the modulation of transmitted or internally reflected light by absorption due to free carriers. See, for example, N. J. Harrick, [J. Phys. Chem. Solids **14**, 60 (1960)].